
BED SCOUR IN CURVED OPEN CHANNELS

By

Atef Abdel -Hameed El-Saiad

Associate Professor at Water and Water Structures Eng. Dept
Faculty of Eng., Zagazig Univ., Egypt.

ABSTRACT

The mechanics of flow in a curved alluvial channel has some distinct characteristics that are absent in a straight alluvial channel. The forces governing the flow are different in nature. The flow is asymmetrical, and an interaction between the secondary current and primary flow produces a spiral flow pattern affecting the transport of sediments. It is generally assumed that the governing forces in a bend flow are the centrifugal forces due to the vertical non-uniformity of the velocity profile combined with the flow curvature, the shear stresses, and the radial pressure gradients caused by transverse inclination of the water surface. The balance between the governing forces tends to produce a helical flow pattern in the bend and a tilting of the channel bed, with an increase in the depth near the outer (concave) bank. As a result, the outer bank is often undermined and eroded. This experimental study have been made to relate these features to mean flow characteristics. The effect of curvilinear flow on scour in two opposite successive bends of central angle 133.29° , the bend radius at center line, $r_c = 20, 22.5, \text{ and } 25\text{cm}$, and the bend width $B=10, 15 \text{ and } 20\text{cm}$. are discussed in this study. Empirical equations have been developed for estimating the maximum scour depth for the two opposite successive bends, the first is called upstream bend and the second is the downstream one.

INTRODUCTION

The behavior of curvilinear flow in curved open channels and rivers has been studied for many years because of its importance in channels and rivers morphology. The movement of sediment plays an important role in deciding the stable geometry of the bed at river bends. The bed load will have a tendency to move towards the inner bank on account of secondary flow. This radial movement of the bed load causes scour near the outer bank (concave bank) and deposition near the inner bank (convex bank). Many investigators have attempted to explain the bed deformation in meandering rivers. The process of scour and deposition at bends in

alluvial streams are reviewed in the following paragraph.

Yen (1970) studied the bed topography effect on flow in a meander. Approximate theoretical analysis indicates that the fully developed, curved channel flow, the transverse slope at a given point on the stabilized bed is directly proportional to the parameter which characterizes the relative importance of fluid inertia against the gravity acting on a particle, moving along the bed. The fact of proportionality lumps the effects of drag, lift, longitudinal bed slope, and friction between the particle and the bed. He found that the bed topography is a function of width-depth ratio, the Froude number and

the ratio of particle fall velocity to the mean flow velocity.

Engelund (1974), and Hooke (1974). Studied the flow and bed topography in channel bends. They analyzed movement of sediment in bends, and employed sediment continuity and transport formulas to predict equilibrium topography. They studied the drag force effect on the bed slope in longitudinal and transverse directions. They studied the scour and deposition pattern at a 90° bend.

Kikkawa et al (1976) studied the characteristics of flow and the bed topography in a curved open channel. He investigated the change of bed profile with time and the stable bed profile. He studied the segregation phenomenon in the curved open channel and found that when the bed load is transported toward the inside, it is reasonable to suppose that smaller size sand particles are conveyed more often than the larger particles, because the smaller ones are more easily transported.

Carson, M. A., and LaPointe, M. F., (1983) investigated a reach of the **Rouge River**, and found that even though the intensity of near-bank primary velocity may be the main control on erosion. Erosion at the outer bank near bend entrances can occur in response to high bank shear stresses associated with the formation of concentrated helical flow.

Struiksma et al (1985) studied the bed deformation in curved alluvial channels. The main result of his study is that it leads to estimates of the wave length and bed oscillation damping rates, however, good agreement with measured data can only be obtained by using a calibration factor in the sediment transport direction equation. From the analysis the conclusion is drawn that the point bar height and pool depth in bends can not be predicted solely from local conditions. A significant part of the lateral bed slope is

due to an overshoot effect induced by the redistribution of the water and sediment motion in the first part of the bend.

Odgaard (1987) assumed that the bed particles are stable in both longitudinal and radial directions but are at incipient motion condition in the longitudinal direction. Such an analysis also led to the conclusion that the lateral slope is proportional to h_c/r_c .

Ikeda et al. (1987) found that sorting of bed material in bends could reduce the maximum equilibrium scour depth as dramatically as 30-40% in the fully developed region of uniformly curved bends.

Yen et al. (1995) conducted five experiments in a laboratory channel bend of central angle 180° , $r_c = 4.0\text{m}$ and $B = 1.0\text{m}$. The bend was connected with upstream and downstream straight reach and they concluded that, the bed deformation and transverse sorting of sediment become significant beginning around section 30° and 15° , respectively. Also, the maximum deposition height takes place between sections 75° and 90° , and the maximum scour depth occurs between sections 165° and 180° .

Kawai and Julien (1996) carried theoretical and experimental study for bed deformation in a bend with attention focused on point bar formation and possible scour near the inner bank in the case of coarse-grained point bars. They found that the maximum scour depth is observed at a bend angle $\alpha = 60^\circ$ near the outer bank and the bed deformation near the outer bank and the inner bank from bend angle $0 < \alpha < 40^\circ$.

DIMENSIONAL ANALYSIS

Using the principals of the dimensional analysis, the different variables affecting

the relative scour depth can be listed in the following equation,

$$\frac{d_s}{H_c} = \phi \left(\frac{B}{H_c}, \frac{r_c}{H_c}, \frac{d_{50}}{H_c}, F_c, \frac{t}{t_0} \right) \quad (1)$$

Where,

B : the channel width

d_s : the maximum depth of scour ,

d_{50} : the mean diameter of bed material

H_c : water depth at center line of the curved channel

r_c : radius of curved channel at the center line

t : time of scour.

t_0 : time of ultimate scour depth

F_c : the Froude number at the center line
 (= $V/\sqrt{gH_c}$)

V : the mean velocity.

g : gravitational acceleration

The experimental data was measured to study the inter relationships among these variables

EXPERIMENTAL WORK

The experiments were conducted in an adjustable meandering rectangular flume of re-circulating type. Water was re-circulating using an inline pump and the flow rate was measured by using pre-calibrated orifice meter. The tailgate at the downstream end of the flume was used to control the depth of flow for each run. The dimensions of the tested meander: bed width (B) = 10, 15, 20cm, with bend radius

(r_c) = 20, 22.5 and 25cm respectively, the meander wave length, (W) = 66.6, 75.0 and 83.34 cm respectively, and the central bend angle (θ) = 133.29° for the tested models as shown in Figure (1). For all tested models the bed slope was kept horizontal and the two sides were vertical. To study the effect of curvilinear flow on scour depth, the bed was covered initially by a uniform sand layer 20-cm thick, and the d_{50} = 0.22mm.

For each run the bed was leveled and the flow was passed through the flume by very low velocity to the required depth. After that the tail gate was opened gradually to give the suitable velocity which cause starting the scour process in bed material.

The maximum scour depth was measured at intervals of 15, 30 and 60 min for each tested model by using the point gauge. The total number of runs were about 200 runs collected from the tested three models.

ANALYSIS AND DISCUSSION

The relationships between the Froude's number at the center of cross section (F_c) and the relative scour depth (d_s/H_c) at different values of (B/ r_c) for the upstream bend of the channel at different times at 15, 30 and 60 minutes, are presented in Figures (2a, 2b and 2c). These figures show that the relative depth of scour (d_s/H_c) increases by increasing the Froude's number at the center line F_c for

$(B/r_c) = 0.5, 0.67$ and 0.80 . Also, the relationships show that for the same values of F_c , the relative scour depth (d_s/H_c) increases by increasing the value of (B/r_c) from 0.5 to 0.8 . This means that as the radius of curvature (r_c) decreases the scour depth increases due to the increasing of the interaction between the secondary current and primary flow that produces a spiral flow pattern affecting the transport of sediments causing scour at the outer bank and deposition at the inner bank. The eddies cause scour depth near the outer side and deposition near the inner side, this results in larger transverse bed slope and therefore the larger particles of bed material can resist the transverse component of bed shear stress more than the finer particles. So, the fine particles are easily transported to the inner bank region as the transverse bed slope increases.

The relationships between the Froude's number at the center of cross section (F_c) and the relative scour depth (d_s/r_c) at different values of (B/r_c) for the upstream bend of the channel at different times of $15, 30$ and 60 min, are shown in Figures (3a, 3b and 3c). These Figures show that the relative depth of scour (d_s/r_c) increases by increasing the Froude's number at the center line F_c for $B/r_c = 0.50, 0.67$ and 0.80 . Also the relationships show that for the same values of F_c the relative

scour depth (d_s/r_c) increases by increasing the value of (B/r_c) . This due to the increasing effects of spiral flow, which interacted with the secondary currents. The experimental results indicate that the maximum deposition height takes place between sections 30° and 120° and the maximum scour depth occurs between sections 10° and 85° for the upstream bend

Figures (4a, 4b and 4c) show the relationship between the Froude's number at the centerline of the downstream bend (F_c) and the relative scour depth (d_s/H_c) at different values of B/r_c at different times $15, 30$ and 60 min. These Figures show that the relative depth of scour (d_s/H_c) increases by increasing the Froude's number at the centerline F_c for $(B/r_c) = 0.5, 0.67$ and 0.80 . Also the relationships show that for the same values of F_c the relative scour depth (d_s/H_c) increases by increasing the value of (B/r_c) from 0.50 to 0.80 .

Figures (5a, 5b and 5c) show the relationship between the Froude's number at the center of cross section (F_c) and the relative scour depth (d_s/r_c) at different values of B/r_c for the downstream bend of the channel at different times $15, 30$ and 60 min. These figures show that the relative depth of scour (d_s/r_c) increases by increasing the Froude's number at the centerline F_c for $B/r_c = 0.5, 0.67$ and 0.80 . Also the relationships show that for the

same values of F_c the relative scour depth (d_s/r_c) increases by increasing the value of B/r_c from 0.50 to 0.80. For the downstream bend the experimental results indicate that the maximum deposition height takes place between sections 40° and 110° and the maximum scour depth occurs between sections 10° and 60° .

The relative scour depth (d_s/H_c) for upstream bend at different values of $B/r_c = 0.5, 0.67, 0.80$, increases by increasing the time from 15min to 60min. The rate of increasing in relative scour depth decreases by increasing B/r_c from 0.50 to 0.80 as shown in Figures (6a, 6b, and 6c).

Figure (7) shows the relationship between the measured and the calculated values of relative scour depth (d_s/H_c) for all tested runs in the upstream bend. This figure shows that the measured values of (d_s/H_c) are in good agreement with calculated values by using the following equation, which has been developed, by using multiple linear technique method.

$$\frac{d_s}{H_c} = 0.045 + 6.08 \frac{H_c}{r_c} + 8.69 F_c^{0.1} - 2.29 \left(\frac{H_c}{B} \right)^{0.5} - 4.26 \left(\frac{H_c}{d_{50}} \right)^{0.1} + 0.18 \frac{t}{t_0} \quad (2)$$

Equation (2) has a regression coefficient $R^2 = 0.77$, and the standard error of estimation (S.E.E) = 0.08

Figure (8) shows the relationship between the measured and the calculated

values of scour depth (d_s/H_c) for all tested runs in the downstream bend. This figure shows that the measured values of (d_s/H_c) are in good agreement with calculated values by using the following equation, which has been developed, by using multiple linear technique method.

$$\frac{d_s}{H_c} = 0.803 + 7.0 \frac{H_c}{r_c} + 9.05 F_c^{0.1} - 3.51 \left(\frac{H_c}{B} \right)^{0.5} - 4.51 \left(\frac{H_c}{d_{50}} \right)^{0.1} + 0.127 \frac{t}{t_0} \quad (3)$$

Equation (3) has a regression coefficient $R^2 = 0.82$, and the standard error of estimation (S.E.E) = 0.09. Equations 2 and 3 can be used for estimating the maximum scour depth at the outer bank of upstream and downstream bend respectively within the following limits, $H_c/d_{50} = 135-360$,

$$d_{50}/B = 1.10 \times 10^{-3} - 2.2 \times 10^{-3},$$

$$B/r_c = 0.50 - 0.80, \quad H_c/B = 0.20-0.88,$$

$$H_c/r_c = 0.02 - 0.20 \text{ and } F_c = 0.15-0.45,$$

$$t/t_0 = 0.25-1.0$$

Figures (9a and 9b) show the distribution of residuals values with the predicted values of d_s/H_c for upstream bend and downstream bend respectively. The residuals are mostly distributed around the line of zero. Residuals with mean = -0.00165, -0.00292, standard deviation S.D. = 0.054, 0.069, and correlation coefficient $r = -0.0139, 0.028$ for upstream and downstream bend respectively. The low

value of correlation coefficient means that the residuals are un-correlated indicating the validity of equations 2 and 3 for estimating the relative scour depth.

Figures (10) and (11) show the relationship between the measured and the calculated values of relative scour depth (d_s/H_c) and the Froude's number F_c for all tested runs of upstream bend and downstream bend. These figures show that the relative scour depth for D.S. bend is bigger than of U.S. bend. This due to the effect of additional eddies and turbulence of coming curvilinear flow from upstream bend.

Illustrative Example

A rectangular open channel of two vertical sides has two successive bends of radius 20.0m in opposite direction. The bed material has mean diameter $d_{50} = 1.10$ cm, the bed width of the channel is 10.0m. The water depth at centerline of the first bend is 2.0m and the water depth at the centerline of second bend is 1.95m. If the discharge through the channel is 20 m³/s. Find the ultimate scour depth at the outer sides of the two bends for $t/t_0 = 1.0$.

Given.

$B = 10.0$ m, $r_c = 20$ m,
 H_c for U.S. bend = 2.0m, ,
 H_c for D.S. bend = 1.95m

$d_{50} = 1.10$ cm, $Q = 20$ m³/s, $t/t_0 = 1.0$

Required: The maximum scour depth for upstream and downstream bend.

Solution:

1- for upstream bend

$$F_c = \frac{V}{\sqrt{gH_c}} = \frac{(20/20)}{\sqrt{9.81 \times 2.0}} = 0.226$$

By using equation 2, then,

$$\frac{d_s}{2.0} = 0.045 + 6.08 \frac{2.0}{20} + 8.69(0.226)^{0.1} - 2.29 \left(\frac{2.0}{10} \right)^{0.5} - 4.26 \left(\frac{2.0}{0.011} \right)^{0.1} + 0.18(1.0)$$

$$\therefore ds = 0.26\text{m}$$

2- for downstream bend

$$F_c = \frac{V}{\sqrt{gH_c}} = \frac{(20/19.5)}{\sqrt{9.81 \times 1.95}} = 0.235$$

By using equation 3, then,

$$\frac{d_s}{1.95} = 0.803 + 7.0 \frac{1.95}{20} + 9.05(0.235)^{0.1} - 3.51 \left(\frac{1.95}{10} \right)^{0.5} - 4.51 \left(\frac{1.95}{0.011} \right)^{0.1} + 0.127(1.0)$$

$$\therefore ds = 0.63\text{m}$$

This example shows that the maximum scour depth at downstream bend is bigger than that of upstream bend due to the decrease of water depth at center line which cause increasing in Froude's number. Also the additional eddies of curvilinear flow from upstream to downstream bend causes increasing in scour depth.

CONCLUSIONS

From the above discussion the following conclusions can be summarized.

- The relative scour depth (d_s/H_c) and (d_s/r_c) increases by increasing the Froude's number F_c at the centerline for $B/r_c = 0.5, 0.67$ and 0.80 . Also for constant values of F_c the relative scour depth d_s/H_c and (d_s/r_c) increases by increasing the value of B/r_c .
- When the radius of curved channel r_c decreases the scour depth increases due to the major effect of crowded curvilinear streamlines, which produces a spiral flow and eddy currents that cause scour at the outer bank and deposition at the inner bank
- Empirical equations 2 and 3 are developed for estimating the relative scour depth for upstream and downstream bend respectively as a function of H_c/r_c , F_c , H_c/B , H_c/d_{50} and t/t_0 .
- The maximum scour depth at the outer side of downstream bend is bigger than that of upstream bend due to the additional eddy currents and turbulence of curvilinear flow which coming from the upstream bend.
- The rate of increasing in relative scour depth decreases by increasing B/r_c from 0.50 to 0.80 .

- The increasing of streamline curvature at the outer side of the bend and the formation of concentrated helical flow, cause the scour in bed material at the outer bank region. Therefore in order to prevent the scour at the outer side, protective structures such as diagonal sills which can be installed on the bottom of the channel near the ends of bends to reduce the disturbance of flow at the outer side.

REFERENCES

- 1- Carson, M. A., and LaPointe, M. F., (1983), "Inherent asymmetry of river meander plan form", J. of Geology, Vol.91, pp.41-55.
- 2- Englund, F. (1974), "Flow and bed topography in channel bends", J. of hyd. Div. ASCE, Vol. 100, No.11, Nov. 1974, pp1631-1648.
- 3- Hooke, R.L.(1974), "Distribution of sediment and Shear stress in a meander bend", Journal of Geology, Vol.83,1975,pp. 543-567.
- 4- Ikeda, S. Yamasaka, M., and Chiyoda, M. (1987), "Bed topography and sorting in bends", J. of Hyd. Eng., ASCE113 (2), pp. 190-206.
- 5- Kawai, S. and Julien, P.Y.(1996), "Point bar deposits in narrow sharp bends", J. of Hyd. Res. , Vol.34, No. 2, pp. 205-218.

- 6- Kikkawa H., Ikeda S. and Kitagawa A. (1976), "Flow and bed topography in curved open channels", ASCE. J. Hyd. Div. Vol.102 pp.1327-1342.
- 7- Odgaard, A. J. (1987), "Stream-bank erosion along two rivers in Iowa.", Water Res., 23(7), 1225-1236.
- 8- Struiksma, N., Olesen, K. W., Flokstra, C. and De Vriend (1985), "Bed deformation in curved alluvial channels", J. of Hyd. Res. Vol. 23 No.1, pp. 57-79.
- 9- Yen C. L. (1970), "Bed topography effect on flow in a meander". ASCE., Vol. 96, No. HY1. pp. 57-73.
- 10- Yen, C. L. and Lee, K.T. (1995), "Bed Topography and sediment sorting in channel bends with unsteady flow", J. of Hyd. Eng. ASCE., Vol. 121, No.

8. pp. 591-599.

NOMENCLATURES

- B : the channel width
 d_s : the maximum depth of scour
 d_{50} : mean diameter of bed material
 F_c : the Froude number at the center line
 ($= Vc/\sqrt{gH_c}$)
 g : gravitational acceleration
 H_c : water depth at center line of the curved channel
 r_c : radius of curved channel at the center line
 t : time of scour.
 t_b : time of ultimate scour depth
 V : the mean velocity.
 W : the meander wave length
 θ : the central bend angle.

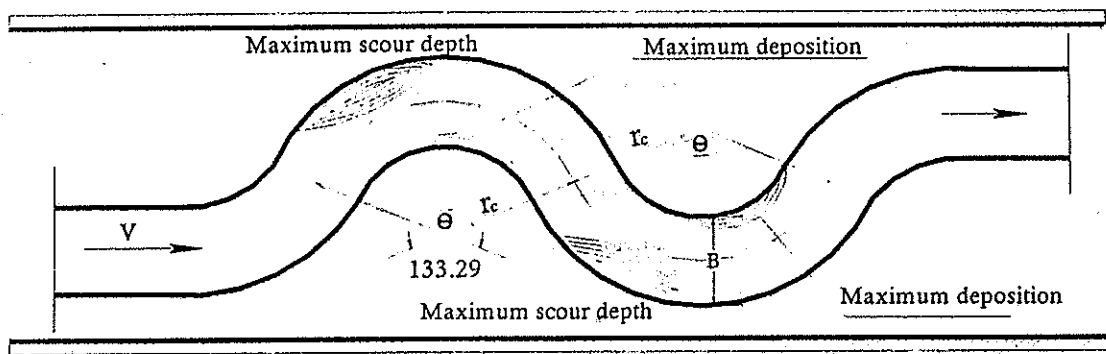


FIG.(1) DEFINITION SKETCH

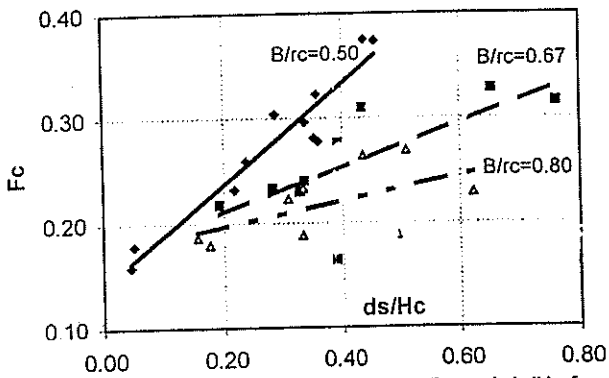


Fig. (2a) The relation between F_c and ds/H_c for upstream bend at time = 15 min.

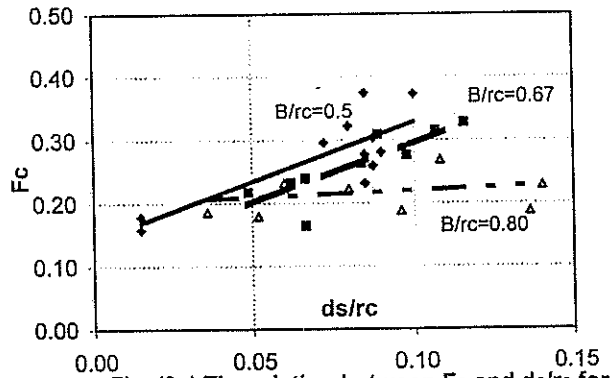


Fig. (3a) The relation between F_c and ds/rc for upstream bend at time = 15 min.

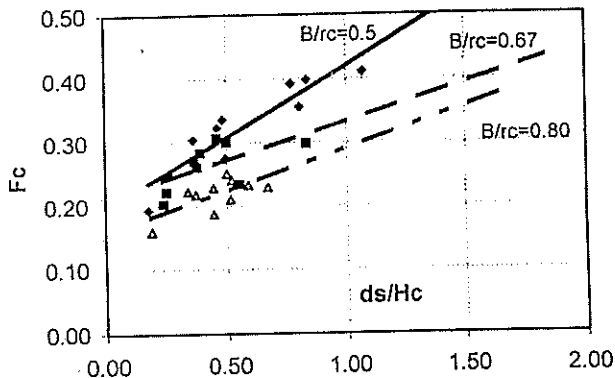


Fig. (2b) The relation between F_c and ds/H_c for upstream bend at time = 30 min.

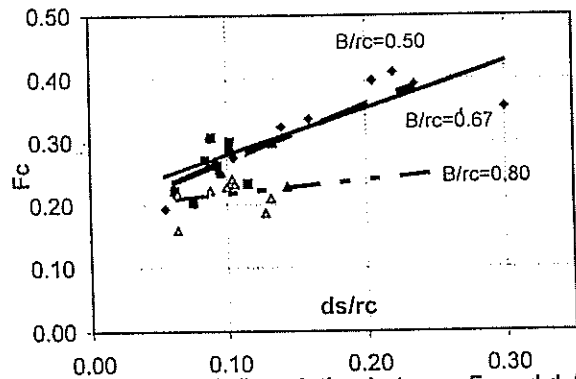


Fig. (3b) The relation between F_c and ds/rc for upstream bend at time = 30 min.

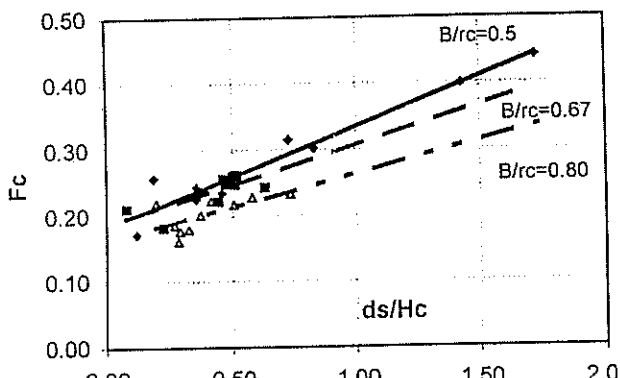


Fig. (2c) The relation between F_c and ds/H_c for upstream bend at time = 60 min.

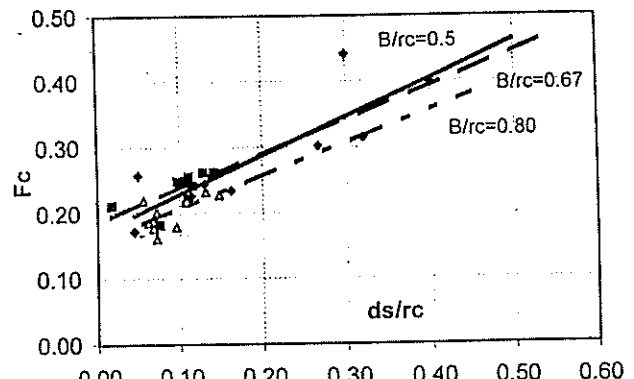
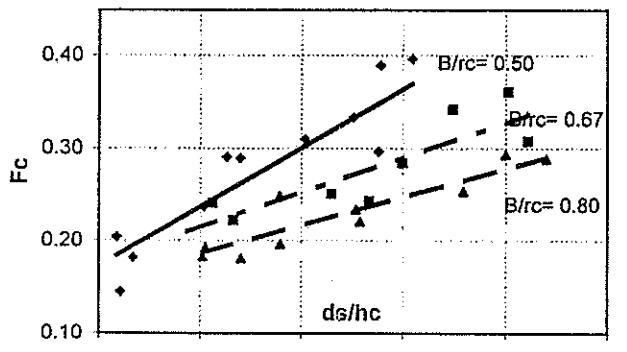
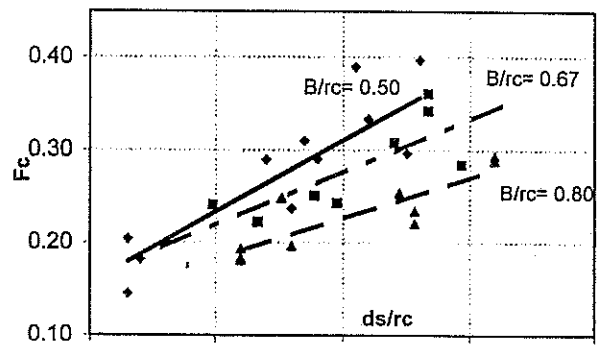


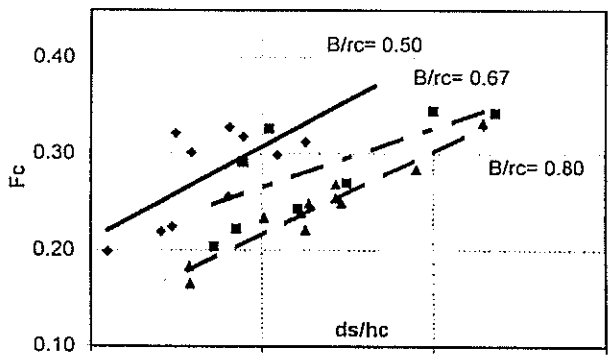
Fig. (3c) The relation between F_c and ds/rc for upstream bend at time = 60 min.



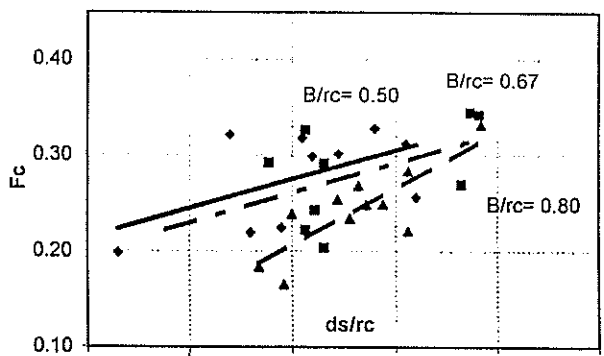
Fig(4a) The relation between F_c and ds/hc for downstream bend at time=15min



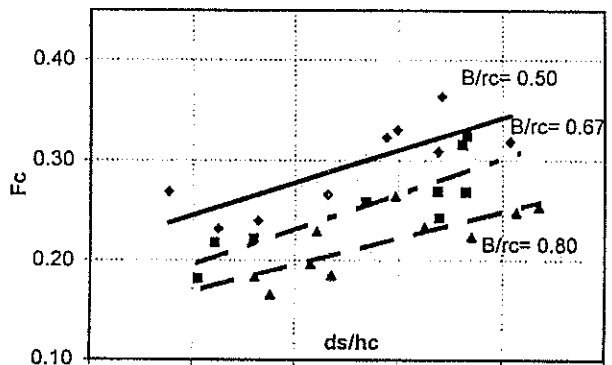
Fig(5a) The relation between F_c and ds/rc for downstream bend at time=15min



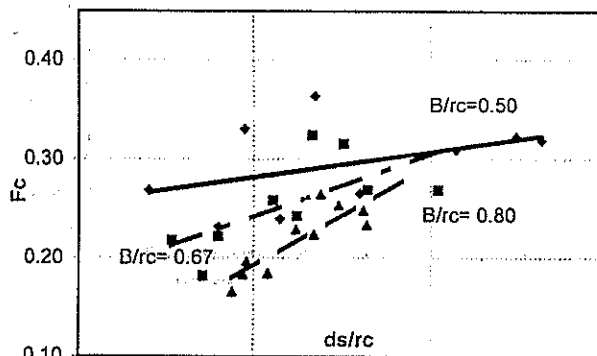
Fig(4b) The relation between F_c and ds/hc for downstream bend at time=30min



Fig(5b) The relation between F_c and ds/rc for downstream bend at time=30min



Fig(4c) The relation between F_c and ds/hc for downstream bend at time=60min



Fig(5c) The relation between F_c and ds/hc for downstream bent at time=60min

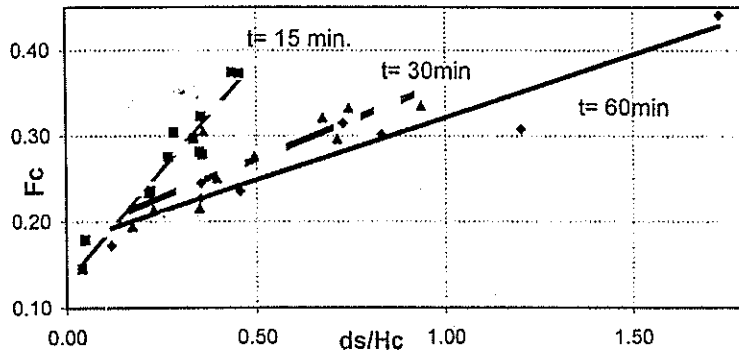


Fig. (6a) The relation between F_c and ds/H_c for $B/rc = 0.5$ at different times for U.S. bend.

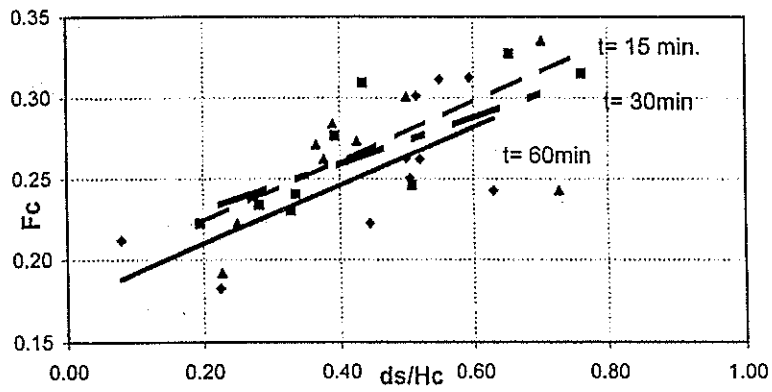


Fig. (6b) The relation between F_c and ds/H_c for $B/rc = 0.67$ at different times for U.S. bend.

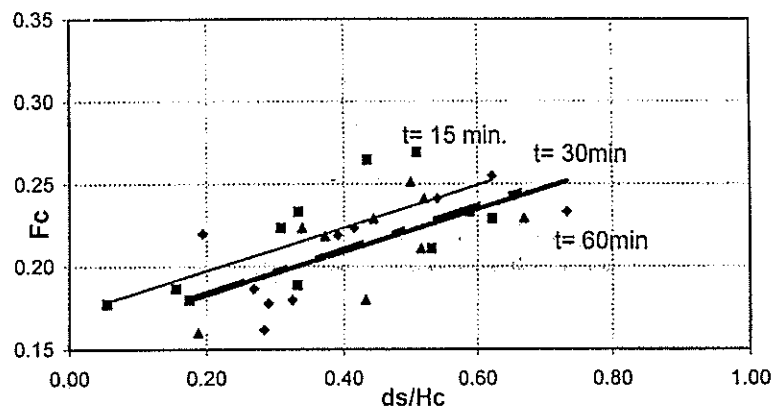


Fig. (6c) The relation between F_c and ds/H_c for $B/rc = 0.80$ at different times for U.S. bend.

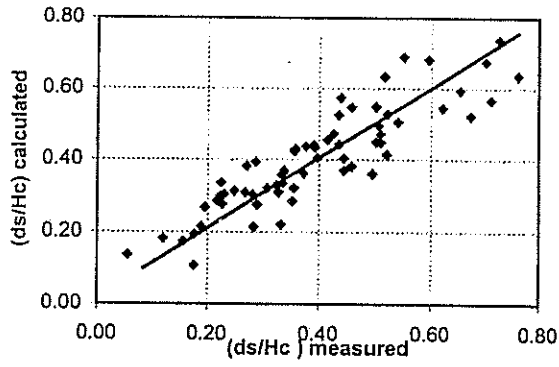


Fig.(7) The relationship between the measured and the calculated values of ds/Hc for U.S bend

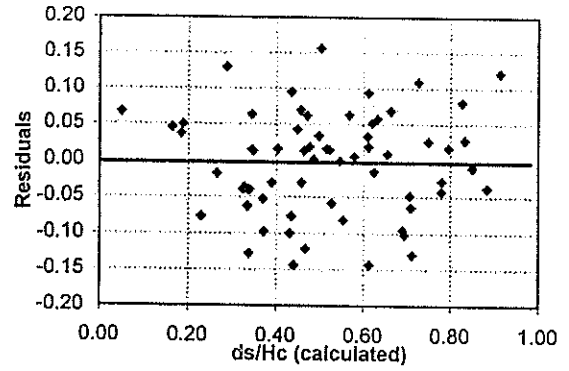


Fig.(9b) Distribution of residuals with the predicted values of ds/Hc for D.S. bend

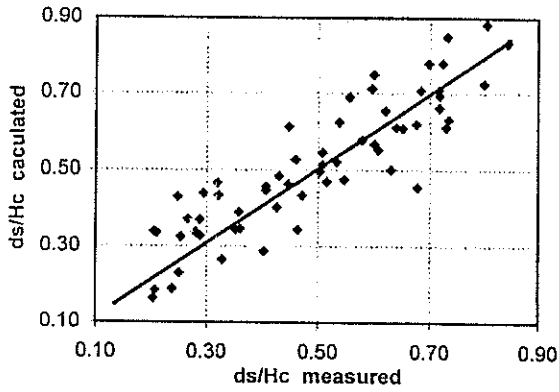


Fig.(8) The relationship between the measured and the calculated values of ds/Hc for D.S bend

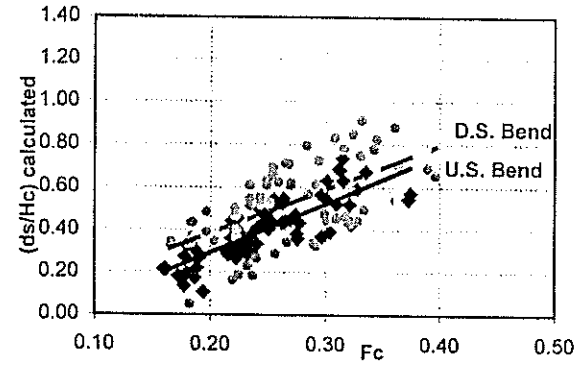


Fig.(10) The relationship between the calculated values of (ds/Hc) and F_c

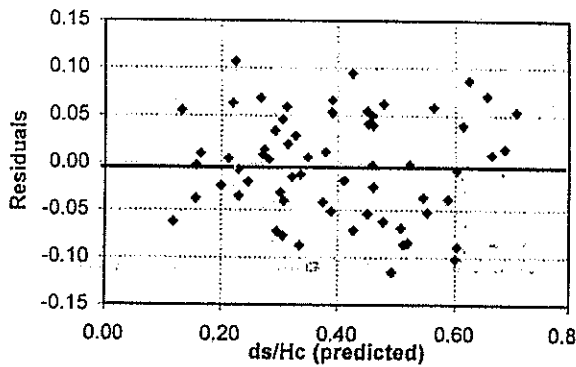


Fig.(9a) Distribution of residuals with the predicted values of ds/Hc for U.S. bend

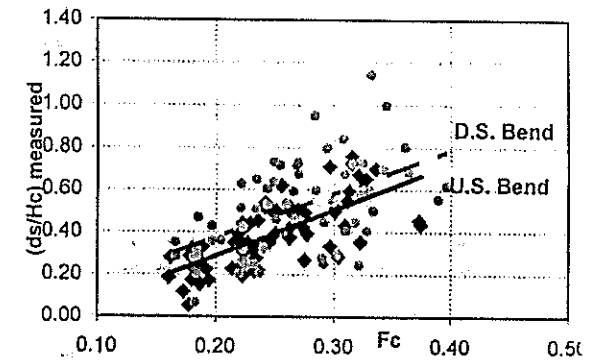


Fig.(11) The relationship between the measured values of (ds/Hc) and F_c